Electronic and geometrical structure of the NF_2 radical

Aristotle Papakondylis and Aristides Mavridis

Laboratory of Physical Chemistry, Department of Chemistry, National and Kapodistrian University of Athens, Panepistemiopolis, Athens 15771, Greece

Received 13 August 1993; in final form 10 September 1993

Ab initio calculations of equilibrium geometries, excitation energies, dipole moments and charges for the low-lying $X\,^2B_1$, $1\,^2A_1$, $2\,^2A_1$, $^2B_2$ and $^2A_2$ electronic states of the NF_2 radical have been carried out at the RHF/SDCI level, using large basis sets. Our results are in good agreement with experimental data. In addition, a rationalization scheme for the experimental results obtained through UV spectroscopy and photolysis of NF_2 is proposed on the basis of our theoretical results.

1. Introduction

The NF_2 radical is easily produced by heating tetrafluorohydrazine, F_2NNF_2 [1]. The molecule has attracted some attention, mainly because the reaction between H and NF_2 produces NF in its $^1\Delta$ excited state, which is radiatively stable with respect to its $^3\Sigma^-$ ground state and thus a potential energy storage [2].

Although there are quite a few experimental papers on the photolysis of the NF_2 radical, the spectroscopy is not transparent. The absorption transition between the ground $X\,^2B_1$ state and the first excited state of NF_2 around 260 nm [3,4] shows some diffuse bands which are considered to be caused by predissociation of NF_2. The photolysis of the radical in the region 240–270 nm has been investigated by tunable UV methods and the quantum yield of the metastable NF ($a\,^1\Delta$) species has been measured [5]. In addition, a series of diffuse bands were found in the region 126–140 nm and in 158–170 nm [6].

The equilibrium geometry of the ground $X\,^2B_1$ state of NF_2 is well documented through microwave spectroscopy [7], but no experimental results have been reported on the geometry of the excited states.

Theoretical ab initio studies reported so far have been performed at the SCF level with rather small basis sets or without polarization functions, concerning mainly the ground $X\,^2B_1$ state and the first $^2A_1$ excited state [8–14]. Recently, two ab initio investigations beyond the SCF level have been reported: a CASSCF analysis of the ground $X\,^2B_1$ potential energy surface by Peterson et al. [15], employing a large 11s7p2d contracted to 7s4p2d basis set, and a study of the low-lying excited states by Cai et al. [16]. Cai et al. report UHF/MP2 calculations for the $X\,^2B_1$, $1\,^2A_1$, $^2B_2$ states of NF_2, and UHF for the $2\,^2A_1$ and $^2A_2$ states using a 6-31G* basis. To the best of our knowledge this is the only ab initio work dealing with the low-lying manifold of the NF_2 molecule. It provides for an accurate geometry of the ground state, and a transition energy $\Delta E_{1\,^2A_1 \leftarrow X\,^2B_1}$ in good agreement with the experimental numbers. But the fact that the $2\,^2A_1$ and $^2A_2$ states were calculated at the UHF level, and all states were spin contaminated, coupled with the use of a rather limited basis set, calls for a reinvestigation of the whole problem.

We report here accurate RHF-CISD calculations using a large basis set and treating uniformly all possible low-lying excited states. Notice that the state characterized as $2\,^2A_1$ is of particular interest because, presumably, it plays an important role in the $NF_2 \rightarrow NF + F$ photolysis.

2. Computational details

For both N and F atoms the Duijneveldt Gaussian basis [17] 10s6p contracted to 4s3p according to

SSDI 0009-2614(93)E1254-E

Raffenetti [18] was used. This was augmented by a double set of 6d polarization functions with exponents (1.65, 0.47) and (3.11, 0.86) for N and F, respectively. The resulting [$(4s3p2d)_{N,F}$] basis of $\approx$TZ quality, contains 75 contracted Gaussian components and produces atomic energies of 1–3 mhartree within the HF limit.

Full, point-by-point, geometry optimizations were carried out at the SCF-RHF and at the singles and doubles excitation configuration interaction level (CISD), out of the HF configuration of the appropriate symmetry (SCF+1+2). The CISD calculations were done by keeping the 1s core electrons for every atom frozen at the SCF level. This valence CISD approach generates a space of $\approx$150000 SACs (spin adapted configurations), and in order to keep our correlated calculations under computational control, an energy threshold selection scheme of $\approx 5\times10^{-6}$ hartree was employed truncating the space to $\approx$40000 SACs. The reduced space produces $\approx$98% of the full-CISD correlation energy as evidenced by a full-CISD calculation for calibrating purposes. Thus, all our reported CISD energies have been corrected to the complete CISD space.

To ameliorate size consistency errors, we also report quadruple excitation results (CI-Q) and "full"-CI results (CI-F), obtained through the Davidson extrapolation formulae [19–21]. The Davidson extrapolated results were used mostly as a guide to our CISD results, rather than as computational results per se.

All computations were done with the MELDF code [22] using exclusively the microVAX-3300 computer at the Physical Chemistry Laboratory.

3. Results and discussion

Our SCF results for the X $^2B_1$, 1 $^2A_1$, 2 $^2A_1$, $^2B_2$ and $^2A_2$ states are presented in table 1, while fig. 1 schematically depicts the first four of these states along with their electron distributions. Table 2 compiles all our correlated results at the CISD, CI-Q and CI-F levels of computation.

Let us first examine the SCF results, table 1. In the X $^2B_1$ ground state, the N–F bond length is predicted to be shorter by $\approx$0.04 Å as compared to the experimental value (table 2), a well-known shortcoming of the HF method, compounded here due to the vicissitudes of the F atom. On the contrary, the bond angle is in excellent agreement with the experimental value. Notice that our absolute HF energy is lower by more than 100 mhartree than the corresponding UHF of Cai et al. [16].

The ground state of NF_2 can clearly be characterized as a π radical, with the symmetry carrying electron localized on the N atom, fig. 1a. At the SCF level the 1 $^2A_1$ excited state is located 4.59 eV above the X $^2B_1$ ground state in good agreement with the experimental value (table 2). The corresponding ΔE value for NH_2 is 1.39 eV [23]. The much higher excitation value of NF_2 as compared to NH_2 can be attributed to the stabilization of the $6a_1$ electron pair with the synchronous destabilization of the $2b_1$ elec-

Table 1
Energy dependences ΔE, equilibrium geometrical parameters, dipole moments μ and net Mulliken charges and overlaps (q, S), for the X $^2B_1$, 1 $^2A_1$, 2 $^2A_1$, $^2B_2$ and $^2A_2$ states of NF_2 at the SCF level

Property	State				
	X $^2B_1$	1 $^2A_1$	2 $^2A_1$	$^2B_2$	$^2A_2$
ΔE [a]	0.0	4.59	5.45	6.10	8.01
R_{N-F} [b]	1.312	1.319	1.460	1.503	1.527
$\angle$FNF [b]	103.5	120.4	142.4	74.4	86.8
μ [c]	−0.268	−0.342	−0.642	−0.030	−0.062
q_N	+0.36	+0.23	+0.03	+0.10	+0.12
S_{N-F}	0.20	0.19	−0.07	0.00	0.00

[a] Energy differences in eV; the absolute SCF energy of the ground $^2B_1$ state is $E_{SCF}=-253.26285$ hartree.
[b] Bond length in Å, angles in deg.
[c] Dipole moments in D.

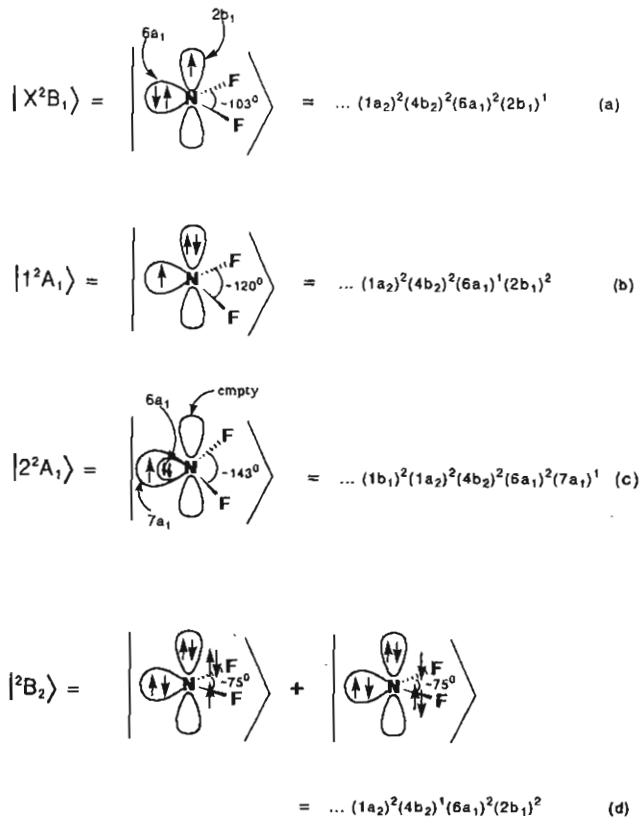

Fig. 1. Schematic SCF representations of the $X\,^2B_1$, $1\,^2A_1$, $2\,^2A_1$ and $^2B_2$ states of NF_2.

tron, due to the presence of the F atoms. It is interesting to note that $\Delta E_{1\,^2A_1 \leftarrow X\,^2B_1}$ is essentially invariant with respect to the level of calculation, table 2. The N–F bond length increases slightly, ≈ 0.01 Å, in going from the $X\,^2B_1$ to the $1\,^2A_1$ state, but the bond angle increases by 17°, also a result independent of the computational level.

A second electronic state of symmetry $^2A_1$, but with different electronic distribution, was found 5.45 eV above the ground state at the SCF level. This state, tagged $2\,^2A_1$, results by promoting the $2b_1$ electron to the $7a_1$ MO, fig. 1c. This is in agreement with the results of Cai et al. [16] who found $\Delta E_{2\,^2A_1 \leftarrow X\,^2B_1} = 5.28$ eV at the UHF level. However, according to our CISD results (table 2) this state is located 4.74 eV above the ground state, 0.17 eV higher than the $1\,^2A_1$ state. In addition, including the Davidson corrections [19–21], the CI-Q and CI-F results suggest that the state $2\,^2A_1$ is below the $1\,^2A_1$ state by ≈ 0.1 and ≈ 0.4 eV, respectively. Due to the possible uncertainties introduced by the Davidson corrections the best we can tell is that these two states of the same symmetry, $1\,^2A_1$ and $2\,^2A_1$, are of the same energy, at least within the resolving power of our calculations.

The geometry of the $2\,^2A_1$ state changes dramatically either with respect to the ground or to the $1\,^2A_1$ state. The N–F bond length increases by as much as ≈ 0.15 Å and the bond angle opens by $\approx 40°$ as compared to the $X\,^2B_1$ state. This drastic geometry change, in conjunction with a zero N–F overlap and a shallow potential energy surface around the minimum, suggests a N–F dissociation channel to the $^3\Sigma^-$ state of the NF species, $NF_2(2\,^2A_1) \rightarrow NF(^3\Sigma^-) + F(^2P)$, fig. 2.

Let us focus now on the correlated results, table 2. For a 19 (valence) electron system such as NF_2, the correlation extracted at the CISD level is $\approx 90\%$ of the total correlation, as is also shown by the Davidson correction to the CI-F energies. Apart from the $^2A_2$ state, bond lengths increase by ≈ 0.01–0.02 Å while bond angles remain practically the same in going from SCF to CISD geometries. The N–F bond length in the $X\,^2B_1$ state is still shorter by ≈ 0.02 Å as compared to the experimental value, but it tends monotonically to the appropriate value after Davidson corrections. We also observe that the calculated dipole moment of the $X\,^2B_1$ state is in fair agreement with the experimental value [7].

At the CISD level the excited states $2\,^2A_1$, $^2B_2$ and $^2A_2$ are compressed by ≈ 0.7, ≈ 0.4 and ≈ 0.8 eV, while, as already mentioned, the $1\,^2A_1$ state remains unchanged. Interestingly enough, at the CI–F level the energy lowering of the previous states becomes twice as large, i.e. ≈ 1.3, ≈ 0.8, and ≈ 1.6 eV, respectively, with respect to the SCF results. We believe that these severe energy lowerings are not real, so we will confine the rest of the discussion to the CISD results.

The two $^2A_1$ potential surfaces are responsible for the creation of an avoided crossing, fig. 3. As a result, the two minima belong to the same symmetry surface, with an intervening energy barrier of, at the most, 8 kcal mol^{-1}, as obtained by a linear geometry variation between the two minima (see fig. 3).

The $^2B_2$ state is created by transferring a $4b_2$ bonding electron to the $2b_1$ nonbonding MO, fig. 1d. The equilibrium geometry of the $^2B_2$ state, table 2, is

Table 2
Energy differences ΔE, equilibrium geometrical parameters, dipole moments μ and net Mulliken charges and overlaps (q, S) for the $X\,^2B_1$, $1\,^2A_1$, $2\,^2A_1$, $^2B_2$ and $^2A_2$ states of NF_2 at the CI level

	Property [a]	State					Exp. [b]
		$X\,^2B_1$	$1\,^2A_1$	$2\,^2A_1$	$^2B_2$	$^2A_2$	
CISD [c]	ΔE [d]	0.0	4.57	4.74	5.72	7.17	4.464 [e]
	R_{N-F}	1.333	1.340	1.477	1.511	1.528	1.3528 [f]
	∠FNF	103.5	120.7	143.1	75.3	89.3	103.3 [f]
	μ	−0.186	−0.211	−0.472	+0.264	+0.350	0.14 [g]
	q_N	+0.28	+0.17	+0.41	+0.02	0.00	–
	S_{NF}	0.17	0.16	0.00	0.00	0.00	–
CI-Q [h]	ΔE	0.0	4.54	4.38	5.49	6.74	
	R_{N-F}	1.347	1.358	1.494	1.536	1.550	
	∠FNF	103.3	120.6	143.2	75.3	90.1	
CI-F [i]	ΔE [j]	0.0	4.51	4.14	5.36	6.48	
	R_{N-F}	1.356	1.367	1.506	1.551	1.574	
	∠FNF	103.2	120.8	143.2	75.4	91.0	

[a] All units as in table 1.
[b] Experimental results for the $X\,^2B_1$ state.
[c] CISD = SCF plus single and double replacements (SCF+1+2).
[d] The absolute CISD energy of the ground $^2B_1$ state is $E_{CISD} = -253.8275$ hartree.
[e] Ref. [24].
[f] Ref. [7].
[g] Absolute value, see ref. [7].
[h] The Davidson correction for the effects of unlinked quadruples, $\Delta E_Q = (1-C_0^2)(E_{CISD}-E_0)$, has been applied, ref. [19]. $E_{CI\text{-}Q}(X\,^2B_1) = -253.8935$ hartree.
[i] The Davidson extrapolation formula to the "full" CI has been used, $E_{CI\text{-}F} = (E_{CISD}-E_0)(C_0^2/2C_0^2-1)+E_0$, refs. [20,21].
[j] The absolute CI-F energy of the ground $^2B_1$ state obtained through the Davidson correction formula given above is $E_{CI\text{-}F} = -253.9020$ hartree.

reminiscent of a N approaching F_2 under C_{2v} symmetry, the F–F bond distance being ≈1.8 Å. We observe that the overlap population for this state is zero for both pairs of atoms. Now, the $^2A_2$ state is created by transferring an electron from a pure fluorine $1a_2$ MO to the $2b_1$ MO of nitrogen, $|...(1a_2)^1(4b_2)^2(6a_1)^2(2b_1)^2\rangle$. This state is the highest in energy among the five states examined here and is unbound with respect to the ground state atoms, $N(^4S)+2F(^2P)$ [25,26]. Both $^2B_2$ and $^2A_2$ states have long bonds, acute angles, no net (Mulliken) charges and reverse dipole moments as compared to the rest of the states, table 2.

In conclusion, we will touch upon the photolysis mechanism of the NF_2 radical in trying to rationalize the experimental results [5].

Fig. 2 shows a diagrammatic representation of the low-lying electronic states of NF_2. It also displays the energy levels of $^3\Sigma^-$, $^1\Delta$, $^1\Sigma^+$ of $NF+F(^2P)$, at the CISD level of calculation. The relative positions of the ground states of NF_2 and $NF(^3\Sigma^-)+F(^2P)$ were determined by using the experimental binding energy of NF_2 (≈6.1 eV) [25,26], and the NF dissociation energy, $D_0 = 3.5$ eV [24].

We summarize the experimental findings: (a) a broad absorption band is observed in the region 240–270 nm or 5.17–4.59 eV with a maximum at ≈260 nm or 4.77 eV [3–5]; (b) the main photolytic product is the $^3\Sigma^-$ state of NF with a small percentage of $^1\Delta$ NF at 260 nm; the percentage of $^1\Delta$ NF increases monotonically to ≈20% at 240 nm. In addition, a delay of the NF production is observed [5]; and (c) there is a diffuse absorption band in the region of ≈160–170 nm or ≈7.8–7.3 eV [6].

Our results, fig. 2, clearly suggest a 270–260 nm transition from the $X\,^2B_1$ to the $1\,^2A_1$–$2\,^2A_1$ states with a facile interconversion between the two minima, followed by the breaking of a N–F bond and the

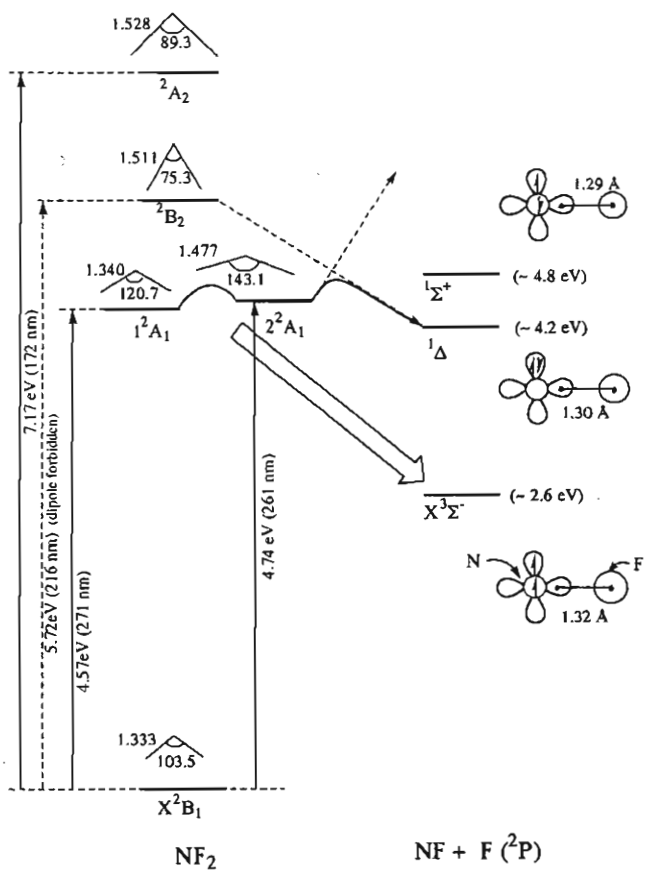

Fig. 2. A photolysis diagram of NF_2 to NF + F. All numbers shown (bond lengths in Å, bond angles in deg) have been obtained through CISD calculations.

production of NF species in the $^3\Sigma^-$ ground state. We can claim that the production of $^1\Delta$ NF is induced by the presence of the $^2B_2$ state; the electronic distribution of the $^2B_2$ state, fig. 1d, is naturally correlated with NF($^1\Delta$) + F(^2P), due to the fact that the in situ N–F fragment in NF_2 is in a $^1\Delta$-like configuration. We infer that increasing the population of antisymmetric b_2 vibrational levels, coupling $^2A_1$ and $^2B_2$ symmetries of NF_2, could result in a partial $^1\Delta$ NF production as shown in fig. 2. In addition, the delay in the $^1\Delta$ NF appearance can be rationalized by the presence of an avoided crossing between surfaces of A′ (C_s) symmetry, resulting from the broken symmetries of $^2A_1$ and $^2B_2$ states.

Finally, the 7.8–7.3 eV transition can be attributed to the $^2A_2 \leftarrow X\,^2B_1$ transition, fig. 2, as suggested by Cai et al. [16].

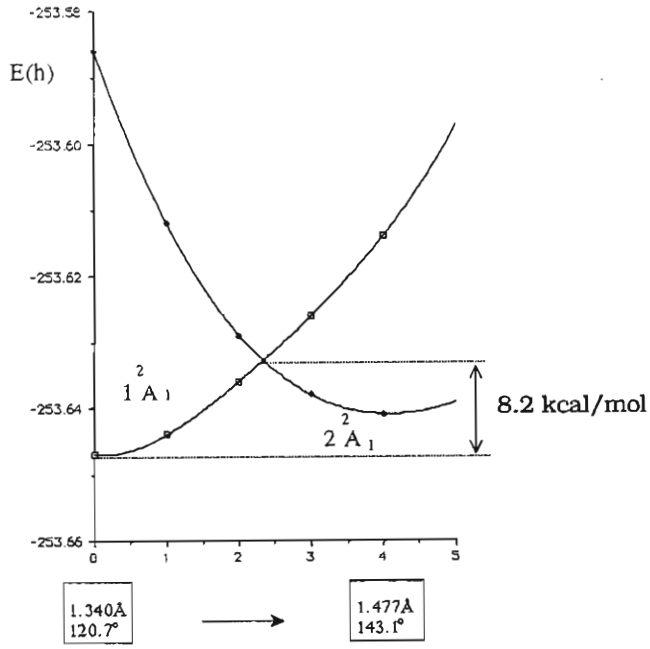

Fig. 3. Avoided crossing of the $1\,^2A_1$ and $2\,^2A_1$ potential energy surfaces of NF_2 at the CISD level.

References

[1] F.A. Johnson and C.B. Colburn, J. Am. Chem. Soc. 83 (1961) 3043.
[2] R.F. Heidner III, H. Helvajian, J.S. Holloway and J.B. Koffend, J. Phys. Chem. 93 (1989) 7818.
[3] P.L. Goodfriend and H.P. Woods, J. Mol. Spectry. 52 (1974) 322.
[4] L.A. Kuznetsova, Y.Y. Kuzyakov and T.M. Tatevskii, Opt. Spectry. 16 (1964) 295.
[5] R.F. Heidner III, H. Helvajian and J.B. Koffend, J. Chem. Phys. 87 (1987) 1520; J. Phys. Chem. 93 (1989) 7813.
[6] R.J. Collins and D. Husain, J. Photochem. 2 (1972) 459.
[7] R.D. Brown, F.R. Burden, P.D. Godfrey and I.R. Gillard, J. Mol. Spectry. 52 (1974) 301.
[8] J.E. Delberne, J. Chem. Phys. 54 (1971) 3487.
[9] C. Thomson and D.A. Brotchie, Chem. Phys. Letters 16 (1972) 573.
[10] S. Rothenberg and H.F. Schaefer III, J. Am. Chem. Soc. 95 (1972) 2095.
[11] R.D. Brown, F.R. Burden, B.T. Hart and G.R. Williams, Theoret. Chim. Acta 28 (1973) 339.
[12] A. Hinchliffe and J.C. Cobb, Chem. Phys. 3 (1974) 271.
[13] A. Hinchliffe and D.G. Bounds, J. Mol. Struct. 54 (1979) 231.
[14] G. Leroy, M. Sana, G. Wilante, D. Peeters and C. Dogimont, J. Mol. Struct. THEOCHEM 153 (1987) 249.
[15] K.A. Peterson, R.C. Mayrhofer and R.C. Woods, J. Chem. Phys. 93 (1990) 5020.